In Silico Polymerization: Computer Simulation of Controlled Radical Polymerization in Bulk and on Flat Surfaces

Jan Genzer*

Department of Chemical & Biomolecular Engineering, North Carolina State University, Raleigh, North Carolina 27695-7905

Received May 22, 2006; Revised Manuscript Received July 17, 2006

ABSTRACT: We use Monte Carlo computer simulation to study the effect of several molecular parameters on controlled/"living" radical polymerization in bulk and on flat substrates. Specifically, we investigate how the molecular weight and molecular weight distribution of grown polymers depend on the initial number of initiators, the initial number of monomers, the initiator activation probability, the initial probability of addition of a new monomer to a growing chain, the probability of terminating two "living" polymers, and the numbers of "living" polymers and their lifetime. Some observations reported here are common to both bulk- and surface-initiated polymerizations. Specifically, we demonstrate that increasing the termination probability and/or decreasing the initial probability of addition of a new monomer to a growing chain broadens the molecular weight distribution. In addition, decreasing the lifetime of the "living" radicals results in polymers with narrower molecular weight distributions. One of the goals of this work is to compare the results of polymerization initiated in bulk with that initiated from flat substrates. Our results reveal that the confinement experienced by the surface-initiated polymers leads to an increased number of early terminations, relative to the bulk-initiated polymerization, which in turn, broadens the molecular weight distribution. This effect is enhanced by increasing the grafting density of the initiators on the surface.

Introduction

Recent developments in controlled radical polymerization (CRP) processes have fueled increased interest in the application of polymeric materials in many new areas of science and technology.[1] CRPs offer the possibility of producing polymers with relatively well-defined properties while at the same time maintaining the simplicity of radical processes.[2] Among the several existing CRP techniques, atom transfer radical polymerization (ATRP), pioneered by Sawamoto[3] and Matyjaszewski,[4] has become one of the most ubiquitous tools for many researchers interested in modifying surfaces in order to tune their chemicophysical properties.[5] ATRP has been shown to provide a convenient means of synthesizing functionalized polymers with well-defined composition, structure, and a reasonably small polydispersity index, relative to the free radical process.[6,7] The key reaction in ATRP is the reversible activation/deactivation process using transition metal (M)/ligand (L) complexes: $P-X + M^{I}X/L \rightleftarrows P^{*} + \mathbf{M}^{II}X_2/L$, where M is usually Cu and X is either Cl or Br. The propagating radical, P*, produced by transferring the halogen atom from the dormant polymer P−X to the $M^{I}X/L$ complex, undergoes polymerization until it is deactivated by the $M^{II}X_2/L$ complex (or terminated). The rapid speed of the activation/deactivation cycles relative to the polymerization rate and the low concentration of the active species (relative to the dormant ones) result in generating polymers with moderately narrow polydispersities (i.e., <1.2). Additional $M^{II}X_2$ is typically added to the reaction mixture in order to shift the reaction equilibrium heavily toward the dormant species and hence to regulate the reaction rate and consequently improve the molecular weight distribution. Utilizing CRP in preparing well-controlled polymers while keeping the polymerization mechanism simple and tolerant to a wide variety of possible side-effects is particularly appealing in applications such as surface-grafted polymer layers, where maintaining stringent polymerization conditions required by other more sophisticated polymerization methods (e.g., ionic polymerizations) causes numerous technical difficulties.[8−10]

Surface-grafted polymer assemblies comprising polymer macromolecules grafted by at least one of their ends to surfaces are commonly referred to as polymer brushes. They play an important role in a variety of applications, including controlling colloidal dispersions, tailoring protein adsorption, or generating responsive surfaces. Polymer brushes can be formed via two methodologies, so-called "grafting onto" and "grafting from" techniques. The "grafting from" method has recently received considerable attention because of its ability to form dense homogeneous layers of surface-anchored homopolymers, block copolymers,[11−13] as well as structures comprising patterned assemblies of homopolymers[14−20] and copolymers.[21] Systems involving gradual variation of the grafting density,[22−24] molecular weight,[25,26] and copolymer composition[27−30] and their combinations[31,32] on a single substrate have also been prepared and studied.[33,34]

One of the drawbacks of the "grafting from" approach is that the structure of the brush very near the substrate is not well understood. Confinement effects and complications associated with monomer and catalyst delivery, as well as chain crowding effects, may have profound influence on the way polymers grow from surfaces. Despite the relatively large body of experimental work on "grafting from" polymerization, our understanding of this confinement effect on the characteristics of polymer brushes is very limited. Most systems studied thus far have involved polymer brushes on convex surfaces, such as nano-/microsized spheres.[35−40] The molecular weight and polydispersity index, measured with size exclusion chromatography on polymers cleaved from nanometer-sized spheres after the polymerization, were found to be close to the bulk values. While polymer brushes have also been grown inside concave substrates, including porous silica,[41] silica capillaries,[42,43] and membranes;[44]

* Corresponding author. E-mail: Jan_Genzer@ncsu.edu. Telephone: +1-919-515-2069.

10.1021/ma061155f CCC: $33.50
Published on Web 08/22/2006

limited information exists about their molecular weights and the polydispersity index. Literature data pertaining to the properties of polymer brushes grown from flat substrates are in most cases restricted to reporting the variation of thickness of the brush layer with altering the initiator structure,[45] initiator grafting density,[46−50] and polymerization conditions;[51] only a few studies reported on molecular weight and molecular weight polydispersity.[21,51]

Unfortunately, probing the near-substrate structure of the brush prepared via "grafting from" polymerization is rather difficult to assess experimentally. To this end, computer simulations and modeling approaches may provide complementary information that is not currently accessible experimentally. While there is vast literature on modeling classical polymerization processes[52,53] and bulk CRP,[54−66] we are not aware of any work that aims at modeling surface-initiated CRP. All modeling of CRP has been performed by utilizing rate equations for the individual polymerization processes (initiation, propagation, and termination) using experimentally available rate constants. While this approach is feasible for modeling bulk polymerization, its application for surface-initiated reaction is not appropriate because it is not straightforward to include the effect of surface geometry and initiator concentration into the rate differential equations. To overcome this problem, we adopt a different approach. Specifically, instead of solving sets of differential equations, we use a molecular simulation approach to model the polymerization reaction. A major advantage of this approach is that both bulk- and surface-initiated polymerization reaction can be represented readily.

The chief purpose of this work is to set up a computer simulation framework facilitating relative comparison of the properties of bulk-grown polymers with those generated by surface-initiated polymerization. Gaining detailed insight into the structure of the brush grown via "grafting from" processes will help us understand how the brush properties in the near-substrate region depend on the geometry of the substrate, density of the initiator, and the characteristics of the polymerization. Such information will ultimately assist in designing experimental conditions, leading to "optimal" and well-controlled "grafting from" polymerizations. As mentioned earlier, different applications require that polymer brushes be prepared on a substrate comprising various geometries, including flat, convex, and concave. Depending on the geometry, the growing chains experience a diverse degree of confinement.[67] While for small spheres the confinement effects are not expected to be too severe, stronger spatial restrictions exist for polymer brushes growing on flat or concave surfaces. In this paper, we deal specifically with flat surfaces because this is perhaps the easiest geometry to model and understand and also because there is already a number of available experimental studies pertaining to this geometry. Extension to other geometries, i.e., convex or concave, is straightforward.

Controlled Radical Polymerization Scheme

References 1 and 7 discuss very thoroughly the general concepts of several controlled radical polymerization (CRP) processes. While the individual polymerizations differ in a few details, one common feature of all schemes is a strong shift of the equilibrium between the active (= "living") and dormant species toward the dormant state; this feature endows CRPs with their controlled nature. While a general type of CRP will be modeled here, our scheme generally describes that of the ATRP, excluding any molecular details of the individual reactions. As depicted in Scheme 1, the CRP involves a set of processes

Scheme 1

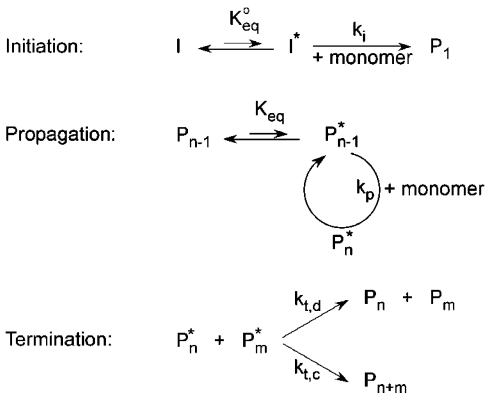

comprising initiation, propagation, and termination steps. While also a transfer step, which involves a radical transfer to another monomer or a solvent, can generally be included, it will not be considered here as this process is heavily suppressed in the CRPs (see below).

As noted by Matyjaszewki,[1] typical attributes of a well-controlled CRP involve a fast initiation step ($k_i \approx 10^5$ L·mol^{-1}·s^{-1}), negligible chain transfer ($k_{tr}/k_p < 10^{-4}$), and a fast termination ($k_t \approx 10^7$ L·mol^{-1}·s^{-1}). The rate of propagation is typically on the order of $k_p \approx 10^{3\pm1}$ L·mol^{-1}·s^{-1}. Because the equilibrium is shifted heavily toward the dormant species ($K_{eq} = k_{act}/k_{deact} \approx 10^{-7}$), there is only a few active macroinitiator radicals (P^*_n) present in the system at a given time ($[P^*_n] \approx 10^{-8\pm1}$ mol·L^{-1}). As a result of the aforementioned attributes, the molecular weight of grown polymer increases linearly with increasing monomer conversion. In addition, the polydispersity index increases slightly at small monomer conversions but decreases steadily at higher monomer conversions. In our molecular model, we cannot use the rate constants (k_x) that are typically employed to characterize the reaction kinetics. Instead, we use reaction and motion probabilities (P_x) to model the molecular steps governing such a polymerization. While it is very challenging to derive conversions between k_x and P_x, we can state that a direct proportionality exists between k_x and P_x. We closely followed this rule when choosing the input values of the P_x parameters in our simulation model. We will demonstrate that the general attributes of CRP mentioned earlier can be reproduced faithfully with our molecular model.

Simulation Model

The Monte Carlo (MC) simulation scheme used to model the "living"/controlled radical polymerization (CRP) is based on the bond fluctuation model (BFM) in the NVT ensemble,[68] where the monomers and polymers reside on a three-dimensional cubic lattice. The allowed set of moves is represented by all possible permutations and sign inversions of the following vector families: **P**(2, 0, 0) ∪ **P**(2, 1, 0) ∪ **P**(2, 1, 1) ∪ **P**(2, 2, 1) ∪ **P**(3, 0, 0) ∪ **P**(3, 1, 0). These vector sets prevent any bond from crossing and monomers (and polymers) from overlapping. Because of its high coordination number, the BFM allows for close approximation of continuum behavior while still offering the advantages of lattice models, such as integer arithmetic and parallelization.[69] While, strictly speaking, the BFM is a coarse-grained model, in this implementation, each bead on the lattice represents an effective monomer unit. The simulation results reported here have been carried out on a cubic lattice $50 \times 50 \times Z$, where Z is either 50 or 100, with periodic boundary conditions applied either in each $X-Y$ plane (surface-initiated polymerization) or all directions (bulk-initiated polymerization).

In the surface-initiated polymerization simulation, the substrate is located at $Z = 1$; the wall opposite to the substrate is modeled as an impenetrable substrate. Most simulations have been carried out on a lattice having $Z = 50$; such a lattice contains $50 \times 50 \times 50 = 125\,000$ sites. Because each effective monomer corresponds to 8 sites, the full lattice occupancy is achieved at 15 625 sites. In some cases involving surface-initiated polymerization, we repeat selected simulation runs for a lattice having $Z = 100$. We comment on these runs in the Results and Discussion Section.

Each simulation run commences with placing the initiators and free monomers on the lattice. In our simulations, the initial number of monomers ($[M]_o$) is set to be either 3125 or 6250, which corresponds to the lattice occupancy of 20% or 40%, respectively. The initial number of initiators ($[I]_o$) is chosen to be either 25 or 100, giving rise to a maximum number of polymers equal to 25 or 100, respectively, that can exist for a given simulation. This number will be reduced during the simulation because of chain termination. This implicit solvent model (no explicit solvent molecules are included in the simulations) is presumed to be valid for modeling the growth of "living" chains under good solvent conditions. As such, this model is expected to mimic very closely most experimental conditions, where there is a very small amount of chain transfer to the monomer. For the bulk-initiated polymerization, the initiator molecules are initially homogeneously distributed throughout the lattice. For the surface-initiated polymerization, the initiators are equidistantly spaced on the substrate ($Z = 1$). After placing the monomers on the lattice, the system is allowed to equilibrate for 10^7 Monte Carlo steps (MCS). The input parameters that determine the polymer growth include: the initiator activation efficiency (P_i), the probability of reaction (growth or termination) vs motion (polymer or a monomer) (P_r), the probability of moving a polymer vs a monomer (P_m), the initial probability of addition of a new monomer to a growing chain ($P_{a,o}$), the probability of terminating two "living" polymers (P_t), the probability of termination via combination ($P_{t,c}$), and the numbers of "living" polymers (FLP) and their lifetime (LT). A general scheme of the individual steps in the computer simulation is depicted in Figure 1. Figure 2 illustrates a flowchart algorithm involving the individual molecular processes, which are described next.

There are two types of polymers present in the system: active and dead. The dead polymers represent those macromolecules that underwent termination; they can only move. The active polymers are either in their dormant or active (= "living") states. The dormant polymers (the number of such polymers is denoted as $[P]_{act,t}$) can only move. Only a fraction of the active polymers is "living" (FLP = fraction of living polymers, or $[P]_{liv,t}$); those can either grow or move. In this simulation, we neglect any molecular details pertaining to any specific CRP mechanism such as the transfer of a halogen atom from the dormant chain to the transition metal/ligand complex, as is done in a real ATRP. Instead, we simply turn the active polymers "on" and "off" in order to make them "living" or dormant, respectively. The FLP is chosen at the beginning of the simulation; typical values are 2, 8, and 16%. The FLP is living for a predetermined lifetime (LT or τ_{lt}) in MCS, again chosen a priori as a constant having a value of either 10^3 or 10^6 MCS. Each MC simulation cycle commences with updating the list of active polymers capable of polymerization. A decision is made based on a generated random number whether a motion or a reaction takes place. Currently, the probability of choosing motion over reaction is fixed during the simulation ($P_r = 0.5$). For simplicity,

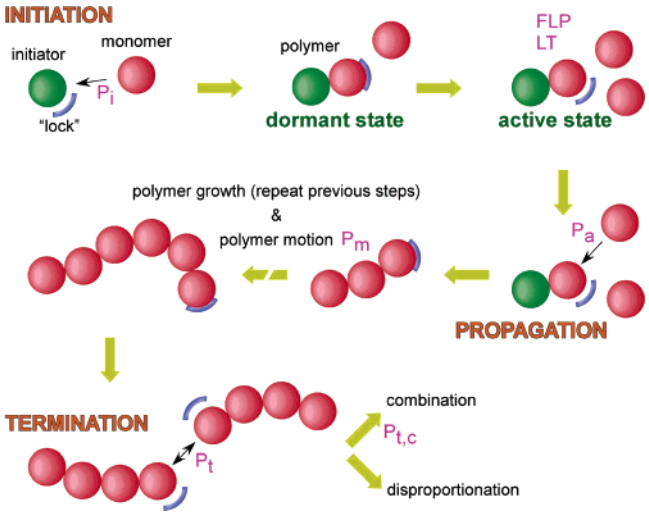

Figure 1. Schematic illustrating the process and parameters used in the MC simulation of controlled radical polymerization. In the initiation stage, the initiator gets activated with the probability of P_i (chosen to be either 0.1 or 1.0). The growing chain resides either in the dormant or active ("living") state. During the simulation, we control the fraction of the "living" polymers (FLP) and their lifetime (LT); both FLP and LT are entered as input parameters at the beginning of the simulation. Several FLP values are simulated (2, 8, or 16%); LT is chosen to be either 10^3 or 10^6 MC steps. Monomer addition occurs only when the chain is in its active/"living" state; the probability of adding a new monomer is P_a; the value of P_a depends on the instantaneous concentration of the monomers ($[M]_t$), the initial number of monomers ($[M]_o$), and a constant $P_{a,o}$, chosen to be either 0.1 or 1.0 ($P_a = P_{a,o}[M]_t/[M]_o$). The polymer may grow or move. Polymer growth may be interrupted via termination, which occurs with the likelihood of P_t when two chains, both in active/"living" state, approach one another with their growing ends to a distance that corresponds to the nearest neighbor distance on the lattice (see text for details). The termination follows either the combination of disproportionation mechanisms. In our simulations we choose the combination via combination ($P_{t,c}$) to occur with the probability of 0.5.

we assume that the rate of motion is equal to the rate of reaction (either propagation or termination). One can thus consider the current model as a simplified version of a kinetic Monte Carlo simulation scheme with fixed reaction and diffusion rates. This is a good approximation because our system is sufficiently dilute so that the viscosity of the solution is not expected to increase considerably during the polymerization.[70]

When motion is selected, either a polymer or a monomer can be moved. The probability of moving a polymer (relative to that of moving a monomer), P_m at time t is given by:

$$P_m = \frac{\sum([P]_t + [M]_t) - \sum([M]_t)}{\sum([P]_t + [M]_t)} = 1 - \frac{\sum([M]_t)}{\sum([P]_t + [M]_t)} \quad (1)$$

where $[P]_t$ and $[M]_t$ are the numbers of polymers and free (= unreacted) monomers, respectively. On the basis of on eq 1, the likelihood of selecting a polymer motion increases with decreasing the number of free monomers. Once the choice of a moving species is made, a polymer (or a monomer) is selected from the list of the existing species (active polymers of monomers) for the motion. If polymer motion is chosen, a monomer along a randomly selected polymer is picked at random for motion along with the moving direction. A check is made as to whether the motion can take place, that is, whether no other species occupies the selected lattice site.

If reaction is chosen, a polymer is selected at random from the list of existing polymers. As stated earlier, only polymers

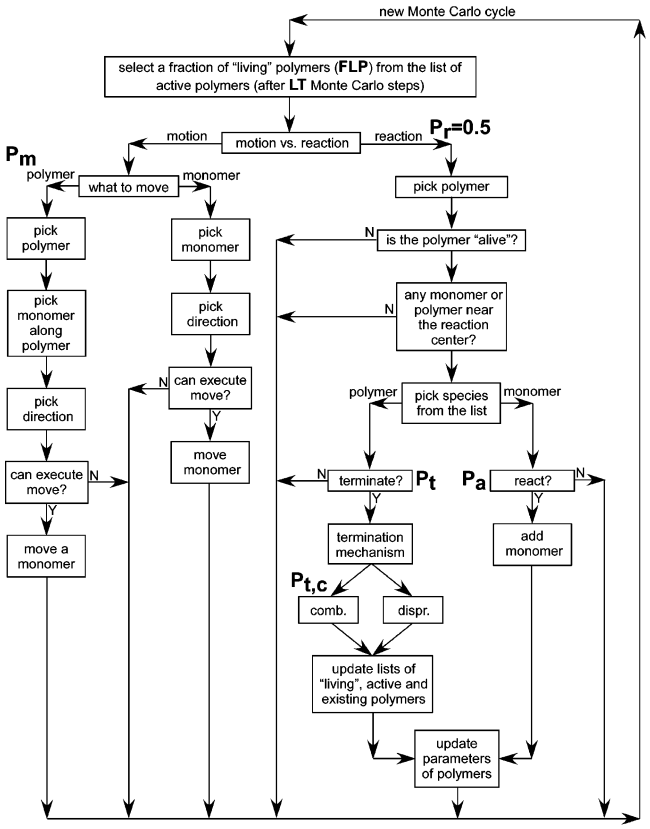

Figure 2. Flowchart depicting the individual steps in the computer simulation modeling of controlled polymerization. Refer to text for details of individual tasks.

that are "living" can react; their number (FLP) is $[P]_{liv,t}$ and their lifetime (LT) is τ_{lt}. After selecting a polymer for reaction, a list of species present in the "neighborhood" of the reactive end group radical on the lattice is generated. The species that count are those that reside within a distance corresponding to a single BFM lattice move (given by the aforementioned set of BMF moves). A species from this list is selected at random, which may react with the "living" radical of the polymer. If the selected species is a radical of another "living" polymer, a termination may take place with a probability P_t. The termination can follow either the combination (probability $P_{t,c}$) or disproportionation (probability $1 - P_{t,c}$) mechanisms. In the simulations presented here, we keep $P_{t,c} = 0.5$. After the termination, we update the number of existing polymers. If termination via combination takes place, the number of existing polymers decreases by 1 and the list of polymers that can be activated decreases by 2. In case of termination via disproportionation, the number of existing polymers does not change, but the number of polymers that can be activated decreases by 2. If the selected species in the list of reactive species is a monomer, propagation takes place with the probability of $P_a = P_{a,o}[M]_t/[M]_o$, where $P_{a,o}$ is an initial addition probability chosen at the beginning of the run (typically, either $P_{a,o} = 0.1$ or $P_{a,o} = 1.0$). Because P_a depends on the instantaneous concentration of free monomers, it decreases with increasing time. When a new monomer is added to the growing polymer, the polymer length increases by 1 and the polymer remains on the list of the "living" species.

A note is necessary to comment on the dormant and active states of the growing polymers. The in silico reaction commences with initiating $[I]_o$ initiators. While we can potentially grow $[I]_o$ polymers, as the polymerization proceeds, some polymers will get terminated, which will reduce both the total number of polymers existing at time t ($[P]_t$) as well as the number of active polymers, $[P]_{act,t}$, so that at any given time $[P]_{act,t} \leq [P]_t$. Out of the total number of active polymers, there are only $[P]_{liv,t}$ macroinitiators "living" at any given time t. Each of these macroinitiators has a lifetime τ_{lt} and a reaction probability equal to P_rP_a. Hence, even if the macroinitiator is active and "living", it will only be able to react for $\tau_{lt}P_rP_a$ lifetime out of its total τ_{lt} lifetime. The lifetime of the macroinitiator (= time during which it can add one more monomer), τ_{act}, is then equal to:

$$\tau_{act} = \frac{[P]_{liv,t}}{[P]_{act,t}}\tau_{lt} \tag{2}$$

We arrived at the aforementioned relation by considering that, if we have $[P]_{liv,t}$ "living" macroinitiators out of the total of $[P]_{act,t}$ active macroinitiators present in the system, each will be activated with the probability equal to $[P]_{liv,t}/[P]_{act,t}$. By multiplying the product of the likelihood of the activation and the lifetime of each macroinitiator, τ_{lt}, we obtain the total lifetime. The dormant (or inactive) state of the macroinitiator, τ_{dorm}, can be derived by simply subtracting the active lifetime of the macroinitiator from the total lifetime, hence:

$$\tau_{dorm} = \frac{[P]_{act,t} - [P]_{liv,t}}{[P]_{act,t}}\tau_{lt} = \left(1 - \frac{[P]_{liv,t}}{[P]_{act,t}}\right)\tau_{lt} \tag{3}$$

Each of these active ("living")/dormant cycles will have a period equal to:

$$\tau_{cycle} = \frac{[P]_{act,t}}{[P]_{liv,t}}\tau_{lt} \tag{4}$$

The above expression means that, statistically, each active polymer will live for time τ_{lt} during one cycle time, τ_{cycle}. Let us further explore the expression given by eq 4. Because in free radical polymerization, $[P]_{liv,t} = [P]_{act,t}$, we have $\tau_{act} = \tau_{cycle} = \tau_{lt}$, $\tau_{dorm} = 0$. Consider now a CRP with 5% "living" macroinitiators, $[P]_{liv,t}/[P]_{act,t} = 0.05$. Using eqs 2−4, we get $\tau_{act} = 0.05\tau_{lt}$, $\tau_{dorm} = 0.95\tau_{lt}$, and $\tau_{cycle} = 20\tau_{lt}$. Because decreasing $[P]_{liv,t}/[P]_{act,t}$ further decreases τ_{act} and increases τ_{dorm}, one would expect the controlled nature of the polymerization to be quite efficient for relatively small values of τ_{lt} (LT) and small values of $[P]_{liv,t}/[P]_{act,t}$ (FLP). Under these conditions, a chance of polymer termination is relatively low.[1]

The MC simulation is allowed to run for a predetermined number of MCS, typically 10^8-10^9. Chain statistics (i.e., molecular weight, polydispersity index) and the coordinates of the monomers of each polymer and all monomers are periodically stored after several thousand MCS. The results presented and discussed here represent averages over 3−5 Monte Carlo simulation runs performed using the same set of input parameters.

Results and Discussion

We pick the following system as our benchmark: the initial number of initiators ($[I]_o$) equal to 100, initial number of monomers ($[M]_o$) equal to 3125, initiator efficiency (P_i) equal to 1.0, initial monomer addition probability ($P_{a,o}$) of 1.0, termination probability (P_t) of 0.1, the fraction of "living polymers" (FLP) equal to 8%, and their lifetime (LT) equal to 10^3 MC steps. Throughout the simulation, we keep the termination probability via combination ($P_{t,c}$) equal to 0.5 and that of the reaction vs motion (P_r) equal to 0.5. In Figure 3a, we plot

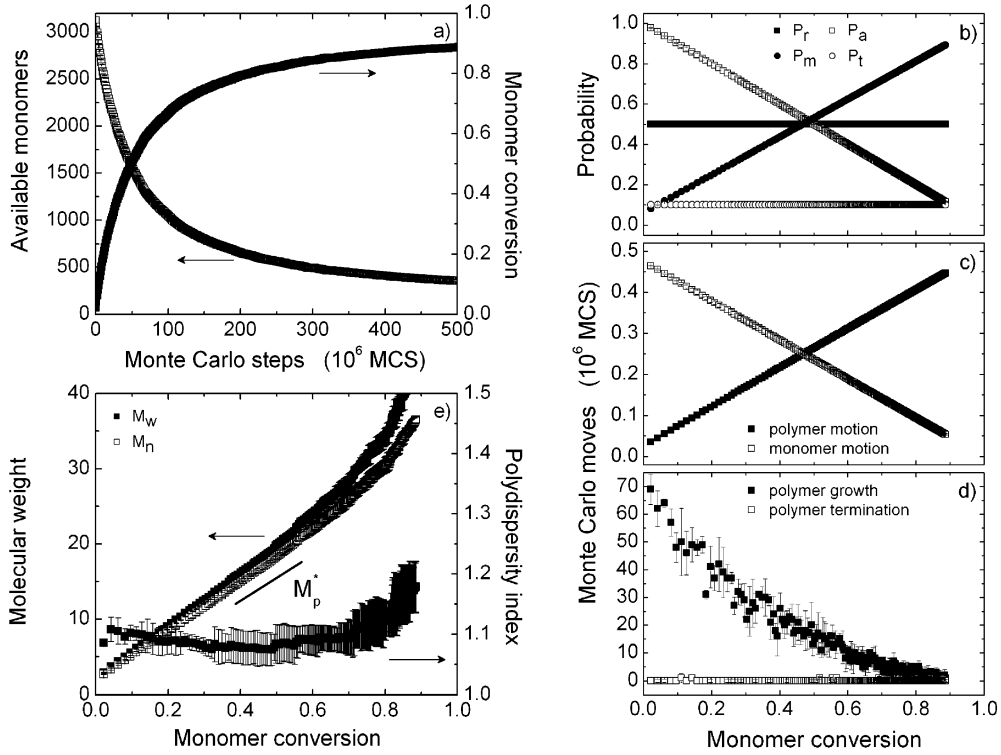

Figure 3. All data presented have been calculated for controlled free radical polymerization in bulk involving the initial number of initiators ($[I]_o$) equal to 100, initial number of monomers ($[M]_o$) equal to 3125, initial monomer addition probability ($P_{a,o}$) of 1.0, termination probability (P_t) of 0.1, the fraction of "living polymers" (FLP) equal to 8%, and their lifetime (LT) equal to 10^3 MC steps. (a) Number of monomers available for polymerization (open symbols, left ordinate) and the monomer conversion (solid symbols, right ordinate) as a function of the number of Monte Carlo steps (MCS). (b) Probability of reaction vs motion (P_r, set to be 0.5), monomer addition (P_a), polymer vs monomer motion (P_m), and termination (P_t, set to be 0.1) as a function of the monomer conversion. (c) Number of MC moves involving polymer and monomer motion as a function of the monomer conversion. (d) Number of MC moves involving polymer growth and polymer termination as a function of the monomer conversion. (e) Weight-average molecular weight (M_w, closed symbols) and number-average molecular weight (M_n, open symbols) as a function of the monomer conversion (left ordinate). The polydispersity index ($= M_w/M_n$, closed symbols) as a function of the monomer conversion (right ordinate).

the instantaneous number of monomers (open symbols, left ordinate) and the monomer conversion (solid symbols, right ordinate) as a function of the number of the Monte Carlo steps (MCS). The monomer conversion is given simply by $1 - [M]_t/[M]_o$. In what follows, we use the monomer conversion as our universal independent variable. In Figure 3b, we plot the various reaction and motion probabilities discussed earlier, i.e., reaction vs motion, monomer addition (P_a), polymer vs monomer motion (P_m), and termination as a function of the monomer conversion. The data in Figure 3b show that the probability of polymer motion (vs monomer motion) increases with increasing monomer conversion, as defined by eq 1. This is further demonstrated by the data in Figure 3c, where we plot the polymer motion (closed symbols) and monomer motion (open symbols) as a function of the monomer conversion. Hence, the larger the polymers become, the more frequently may one of their segments move to a new position. Physically, the condition given by eq 1 states that, on average, each monomer is selected for motion with roughly the same probability, regardless of whether it is free of whether it is a part of a polymer. That, of course, does not always happen, as monomers, which are a part of a growing polymer, cannot move as freely as free monomers because of monomer connectivity constraints in polymers. The data in Figure 3a also depict that the probability of propagation decreases with increasing monomer conversion because the likelihood of adding a new monomer decreases as the number of available monomers decreases with time. In real systems, one tends to work with a large excess of monomer, hence the addition probability would likely stay more or less the same. However, as described below, most of our data refer to relatively small monomer conversions (0.3−0.5, depending on the system), so that even here, the probability of adding a new monomer is still relatively high. In Figure 3d, we compare the rate of polymer growth vs rate of polymer termination as a function of the monomer conversion. While the former steadily decreases, the latter tends to fluctuate about a small number.

By analyzing the properties of the growing polymers, one can obtain information about their molecular weight distribution and polydispersity index, which represents a measure of the breath of the molecular weight distribution. In Figure 3e, we plot the weight-average molecular weight (M_w, closed squares, left ordinate) and the number-average molecular weight (M_n, open squares, left ordinate) as a function of the monomer conversion. To convert from the degree of polymerization (i.e., the number of monomers in each polymer), we assume a unity molecular weight of each monomer. In the same figure, we also plot the polydispersity index ($= M_w/M_n$) (right ordinate) as a function of the monomer conversion. In a well-controlled polymerization process, M_n increases linearly with increasing monomer conversion; the slope of this dependence is a measure of the expected average molecular weight of the polymer (M_p^*). Any deviation from the linear dependence is a sign of an uncontrolled polymerization process.[1] In the Supporting Information, we provide the values of M_p^* for various combinations of $[I]_o$, $[M]_o$, P_i, $P_{a,o}$, P_t, FLP, and LT for both bulk- and surface-initiated polymerizations.

The data in Figure 4 depict the number of polymers (a, d), number of terminations (b, e), and the average radii of gyration of all chain in the ensemble (c, f) for two bulk-initiated

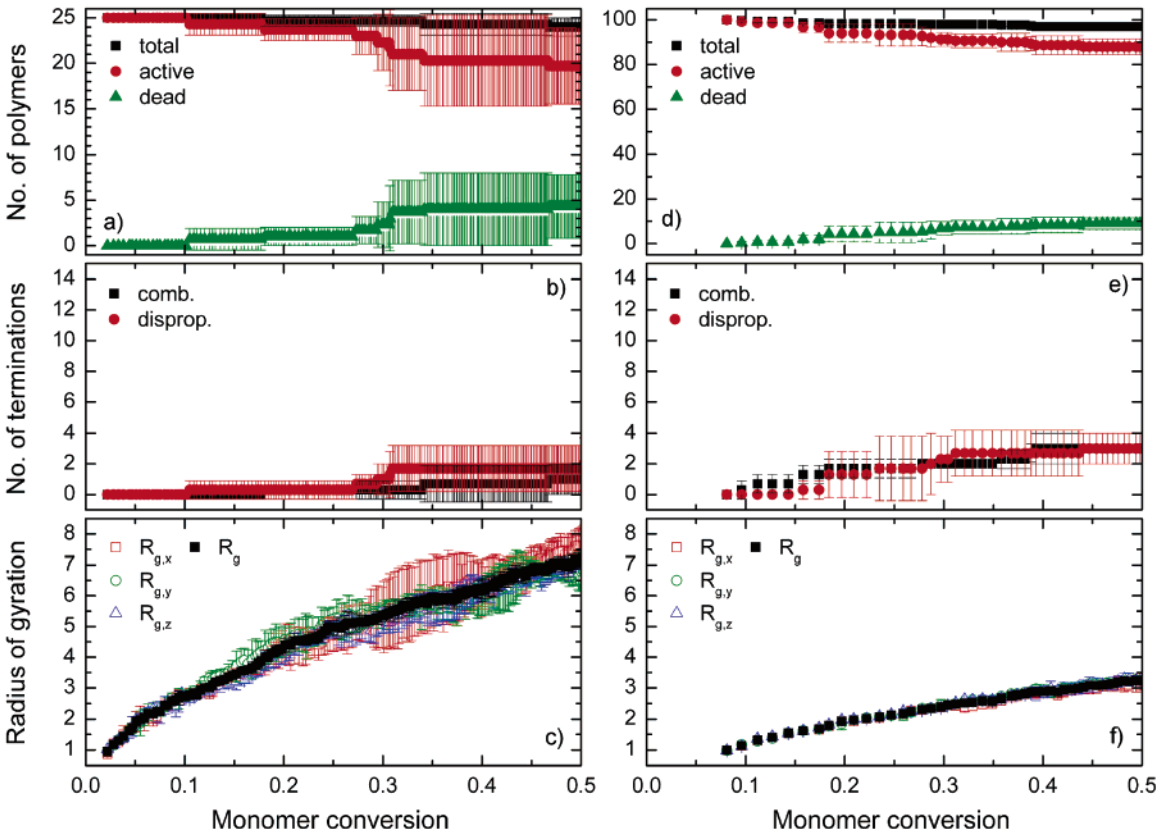

Figure 4. (a, d) Number of polymers (total, alive, and dead), (d, e) number of terminations (combinations and disproportionations), and (c, f) radius of gyration ($R_{g,x}$, $R_{g,y}$, $R_{g,z}$, and R_g) as a function of monomer conversion for the initial number of initiators ($[I]_o$) equal to 25 (left panel, parts a−c) and 100 (right panel, parts d−f) in bulk-initiated controlled radical polymerization. All data have been calculated for the initial number of monomers ($[M]_o$) equal to 3125, initial monomer addition probability ($P_{a,o}$) of 1.0, termination probability (P_t) of 0.1, the fraction of "living polymers" (FLP) equal to 8%, and their lifetime (LT) equal to 10^3 MC steps.

polymerizations having $[I]_o$ equal to 25 (left panel, a−c) and 100 (right panel, d−f) as a function of the monomer conversion.[71] All data have been calculated for the initial number of monomers ($[M]_o$) equal to 3125, initial monomer addition probability ($P_{a,o}$) of 1.0, termination probability (P_t) of 0.1, the fraction of "living polymers" (FLP) equal to 8%, and their lifetime (LT) equal to 10^3 MCS. The trends seen in both low and high initiator concentration cases are very similar. An increase in monomer conversion leads to increases in both the polymer length and the number of terminations. The latter trend results in an increased number of dead chains, which in turn, decreases both the number of active chains, i.e., those that can switch between the dormant and active states, and the total number of polymers. The major difference between the two cases is the length of the growing polymer. Specifically, as expected, decreasing the number of initiators produces longer polymers because $M_p^* = [M]_o/[I]_o$. This feature is demonstrated by the larger polymer radius of gyration for the $[I]_o = 25$ case (Figure 4c) relative to the $[I]_o = 100$ case (Figure 4f). The data in Figure 4c and f also demonstrate that the average dimension of the coil (averaged over all coils present in the ensemble), represented by the respective average radii of gyration along the *X*, *Y*, and *Z* axes, is the same in all lattice directions.[71] Now that we have described the major features of the bulk-initiated polymerization, we compare these findings to the surface-initiated processes. For comparison purposes, we keep all molecular parameters unchanged.

In Figure 5, we plot the number of polymers (a, d), number of terminations (b, e), and the radii of gyration (c, f) for two surface-initiated polymerizations having $[I]_o$ equal to 25 (left panel, a−c) and 100 (right panel, d−f) as a function of monomer conversion. As previously, all data have been calculated for the initial number of monomers ($[M]_o$) equal to 3125, initial monomer addition probability ($P_{a,o}$) of 1.0, termination probability (P_t) of 0.1, the fraction of "living polymers" (FLP) equal to 8%, and their lifetime (LT) equal to 10^3 MC steps. While the trends in the parameters for the surface-initiated polymerization (cf. Figure 5) resemble closely those detected for the bulk-initiated polymerization (cf. Figure 4), some differences exist. Let us begin discussing the $[I]_o = 25$ case first (left panels in Figures 4 and 5). Here, the number of terminations detected in both bulk- and surface-initiated polymerizations is approximately equal, giving rise to a roughly equivalent decrease in the number of active chains and the total number of polymers. The major difference between the two types of polymerizations exists in the coil dimension along different lattice directions. As discussed previously, in the bulk-initiated polymerization, the size of the growing polymer is approximately the same in all three lattice directions. In contrast, the size of the growing polymer brush in the direction away from the surface (*Z* coordinate on the lattice) is much larger than those in *X* and *Y* directions. This behavior is associated with polymer stretching away from the surface in order to avoid "excluded volume" interactions with its in-plane neighbors. As a consequence, the coil is no longer a sphere; it assumes a "football"-like shape. A large difference between the bulk- and surface-initiated polymerization is seen when comparing the polymerization initiated with $[I]_o = 100$ (right panels in Figures 4 and 5). Namely, for the surface-initiated polymerization, there is a very dramatic increase in the number of terminations at low monomer conversion, which is followed by saturation in the number of terminated polymers at higher monomer conversions. This leads

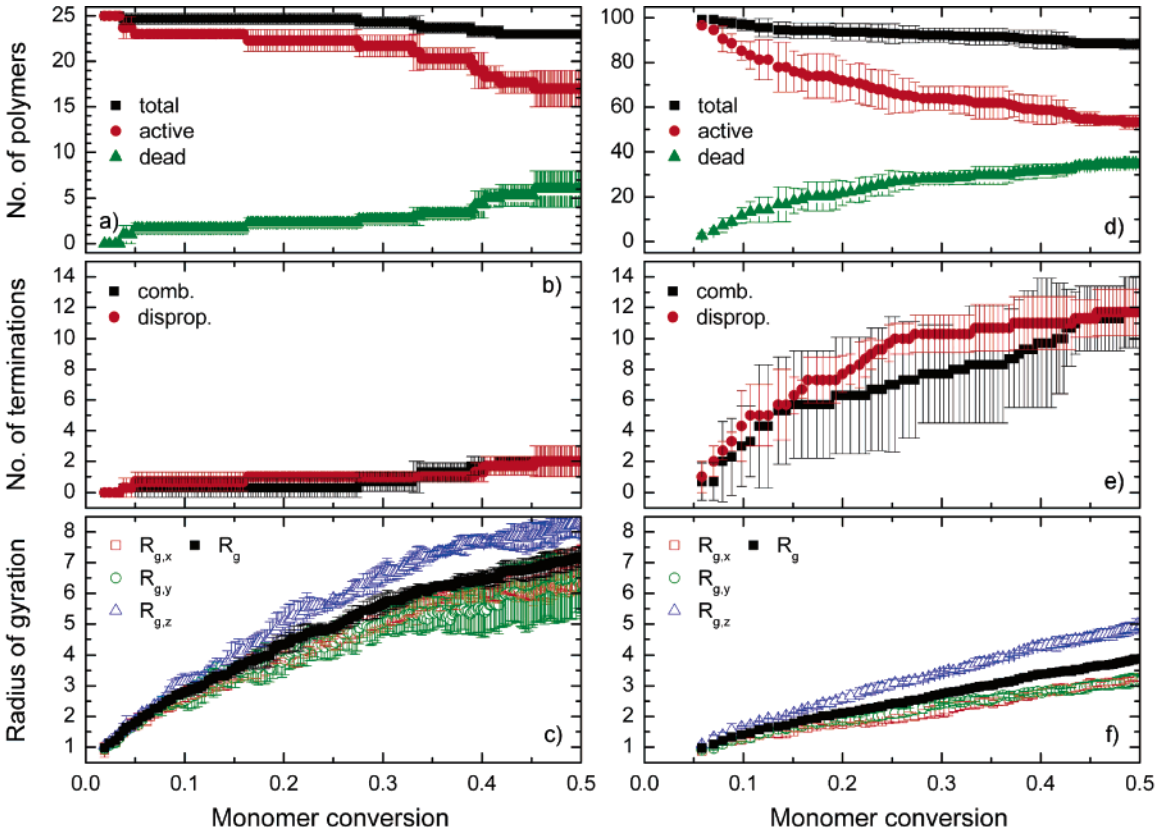

Figure 5. (a, d) Number of polymers (total, alive, and dead), (d, e) number of terminations (combinations and disproportionations), and (c, f) radius of gyration ($R_{g,x}$, $R_{g,y}$, $R_{g,z}$, and R_g) as a function of monomer conversion for the initial number of initiators ($[I]_o$) equal to 25 (left panel, parts a−c) and 100 (right panel, parts d−f) in surface-initiated controlled radical polymerization. All data have been calculated for the initial number of monomers ($[M]_o$) equal to 3125, initial monomer addition probability ($P_{a,o}$) of 1.0, termination probability (P_t) of 0.1, the fraction of "living polymers" (FLP) equal to 8%, and their lifetime (LT) equal to 10^3 MC steps.

to an increased number of dead chains and consequently a decreased number of active chains and the total number of polymers present. The lager number of terminations detected in the surface-initiated polymerization relative to the bulk growth stems from the confinement of the initiators and hence the growing polymers on the surface. Because of this effect, the number of terminations that occur relatively early in the polymerization is dramatically increased relative to the bulk polymerization. Here, a nonnegligible fraction of polymers gets terminated and only a few polymers continue to grow. There is still an increase in the dimension of the growing polymers in the direction away from the surface, as revealed by the comparison of the average radii of gyration in the three lattice directions (again averaged over the entire ensemble). Before we comment in more detail on the differences between the bulk- and surface-initiated polymerizations, let us first explore the effect of those parameters that give rise to the controlled nature of the polymerization, namely the fraction of living polymers (FLP), their lifetime (LT), and their interplay with the probability of termination (P_t) and the initial addition probability ($P_{a,o}$). We do so by monitoring the polydispersity index, as this parameter offers good quality information about the molecular weight uniformity of the grown polymers.

In Figure 6, we plot the polydispersity index as a function of the monomer conversion for bulk-grown polymers using $[I]_o = 100$, $[M]_o = 3125$, having a variable fraction of living polymers (FLP) equal to 2% (top panel), 8% (middle panel), and 16% (lower panel) and their lifetime (LT) equal to 10^3 MCS (left panel) and 10^6 MCS (right panel). In all cases, we keep $P_{a,o} = 1$ and explore the effect of termination probability by varying P_t: 0.01 (red closed symbols), 0.10 (green open symbols), and 1.0 (blue crossed symbols). A first glimpse at the data reveals that, in each case, the polydispersity index decreases with decreasing the probability of termination, as expected. While there does not seem to be substantial differences between the 1% and 10% termination cases, large increases in termination, and hence broadening of the molecular weight distribution, occur by setting $P_t = 1$. For $P_t = 0$, one would anticipate that the molecular weight of the growing polymers is very close to the expected molecular weight M_p^* ($= [M]_o/[I]_o$). This is indeed the case, as demonstrated by the results presented in the Supporting Information. Earlier in the paper, we discussed that polymers with low polydispersities should be produced at low LT and low FLP because, under these conditions, the active time of the "living" chain is minimized (cf. eq 2) and concurrently the residence time of the dormant chain is maximized (cf. eq 3). From the data in Figure 6, for a given FLP, decreasing the LT parameter indeed improves the chain polydispersity. Similarly, we would expect that decreasing FLP also improves chain polydispersity. This does not seem to be the case, as the data in Figure 6 demonstrate. For a given FLP value, all chains seem to have about the same polydispersity indices at given monomer conversions. This behavior may be due to the finite size of our system. Strictly speaking, the conditions presented in eqs 2 and 3 are expected to be valid for systems with millions of growing polymers; hence, even when a small fraction of the polymers, say 1% or less, is living, this number is still much larger than the FLP in our system, where we deal with ≤100 polymers. Despite this technical limitation, the functional dependence of the polydispersity index on the monomer conversion follows the same exact trends, which are detected under

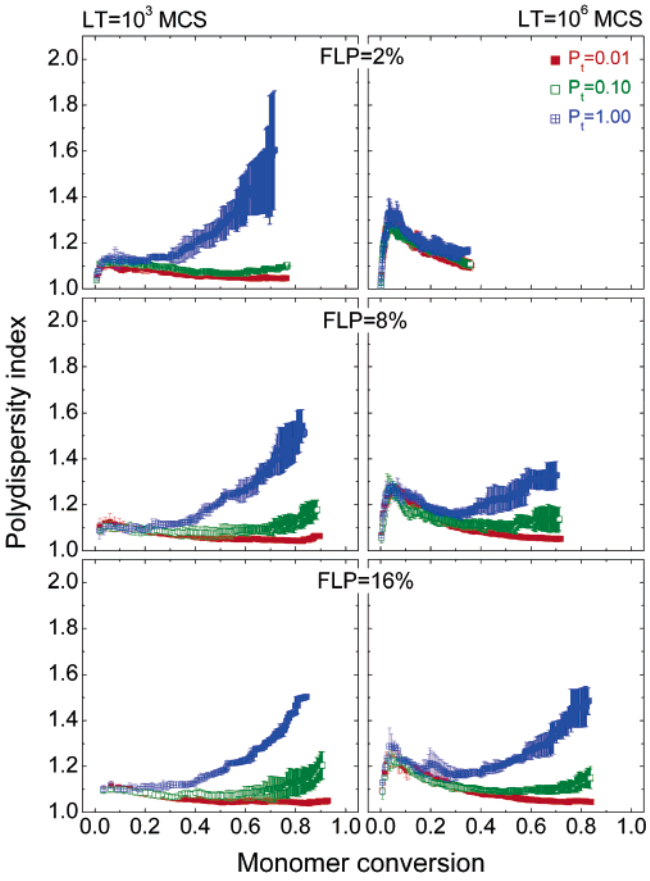

Figure 6. Polydispersity index as a function of the monomer conversion for the bulk-initiated controlled radical polymerization with living polymer lifetime (LT) of 10^3 (left panel) and 10^6 (right panel) for various fractions of the living polymers equal to 2% (top), 8% (middle), and 16% (bottom) and different probabilities of terminations equal to 0.01 (red solid symbols), 0.10 (green open symbols), and 1.0 (blue crossed symbols). All data have been calculated for the initial number of initiators ($[I]_o$) equal to 100, the initial number of monomers ($[M]_o$) equal to 3125, and the initial monomer addition probability ($P_{a,o}$) of 1.0.

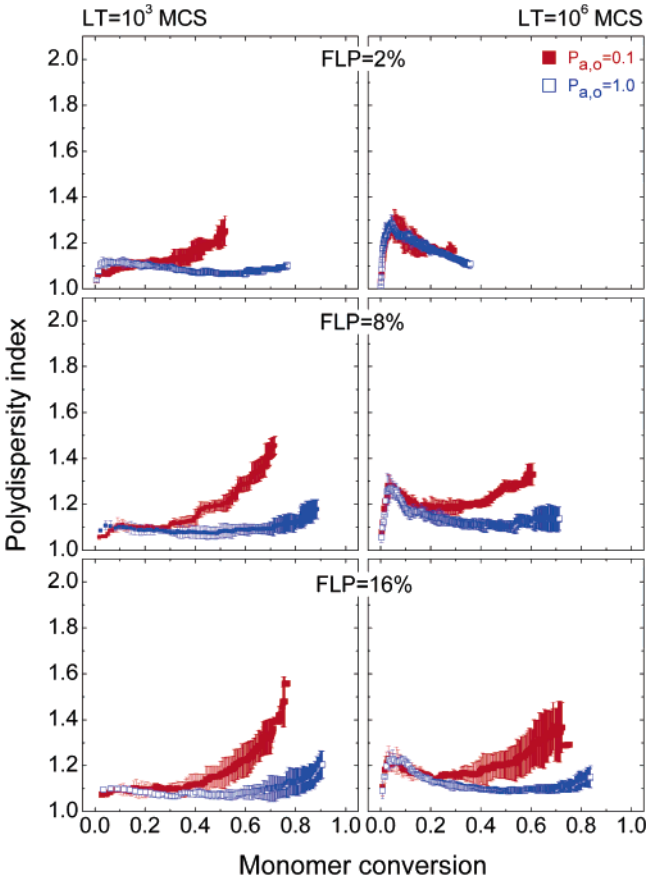

Figure 7. Polydispersity index as a function of the monomer conversion for the bulk-initiated controlled radical polymerization with living polymer lifetime (LT) of 10^3 (left panel) and 10^6 (right panel) for various fractions of the living polymers equal to 2% (top), 8% (middle), and 16% (bottom) and different probabilities of the initial monomer addition probability ($P_{a,t}$) equal to 0.10 (red closed symbols), and 1.0 (blue open symbols). All data have been calculated for the initial number of initiators ($[I]_o$) equal to 100, the initial number of monomers ($[M]_o$) equal to 3125, and the probability of termination (P_t) of 0.1.

real experimental conditions, namely an initial raise at small monomer conversions, followed by a decrease at higher monomer conversions.[1] In radical polymerizations, the polydispersity index is also influenced by the rate of addition of a new monomer to the growing chain. In Figure 7, we present the effect of $P_{a,o}$ for chains growing from $[I]_o = 100$, $[M]_o = 3125$, $P_t = 0.1$, and the same combinations of LT and FLP shown in Figure 6. While there does not seem to be any substantial effect of $P_{a,o}$ on the chain polydispersity at low monomer conversions, at higher monomer conversions, the polydispersity is improved with increasing $P_{a,o}$, as expected.

We now turn our attention to the surface-initiated polymerization and explore the aforementioned effects of LT and FLP on the polydispersity index. For comparison purposes, we perform the simulations with the same set of parameters we used for modeling the bulk-initiated polymerization case. In Figure 8, we plot the polydispersity index as a function of the monomer conversion for $[I]_o = 100$, $[M]_o = 3125$, a variable FLP equal to 2% (top panel), 8% (middle panel), and 16% (lower panel), and LT equal to 10^3 MCS (left panel) and 10^6 MCS (right panel). In all instances, we set $P_{a,o} = 1$ and explore the effect of termination probability by varying P_t: 0.01 (red closed symbols), 0.10 (green open symbols), and 1.0 (blue crossed symbols). By comparing the data in Figures 6 and 8, the trends in the polydispersity index of surface-initiated polymers mimic those reported earlier for the bulk-initiated polymerization. Namely, regardless of the combination of FLP and LT, we detect an increase of chain polydispersity with increasing P_t. These increases are much larger than those seen for the bulk-initiated polymerization. Clearly, the surface confinement of the initiators and the growing polymers has a strong influence on chain polydispersity. Relative to the bulk-initiated polymerization, the polydispersity index increases substantially in the surface-initiated polymerization. This behavior is a consequence of the early chain termination reported previously in Figure 5. As in the bulk-initiated case, decreasing LT leads also here to lowering of the polydispersity index; however, the effect is not as strong. Also, the influence of varying FLP on chain polydispersity is not large. Again, we speculate that the finite size of our system may have influenced our simulated results, as it did in the case of the bulk-initiated polymerization. To summarize these observations, it is clear that the chain polydispersity in surface-initiated polymerizations is larger than that in bulk-based polymerizations carried out under identical conditions. There may be several reasons for this behavior. First, the number of monomers available for reaction may affect the chain growth. Decreasing the number of available monomers decreases the probability of addition, resulting in increases of termination rates. The monomer distribution on the

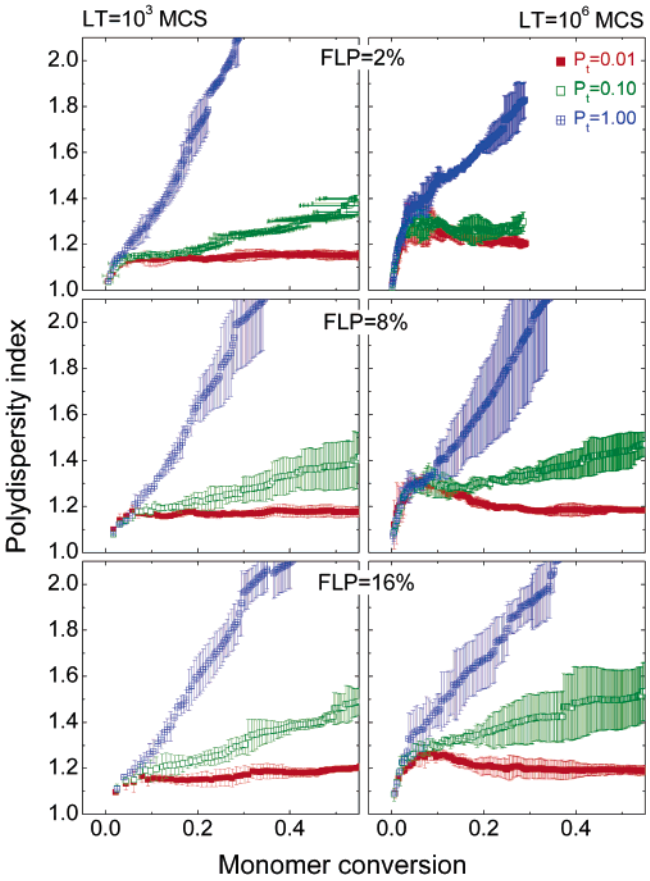

Figure 8. Polydispersity index as a function of the monomer conversion for the surface-initiated controlled radical polymerization with living polymer lifetime (LT) of 10^3 (left panel) and 10^6 (right panel) for various fractions of the living polymers equal to 2% (top), 8% (middle), and 16% (bottom), and different probabilities of terminations equal to 0.01 (red solid symbols), 0.10 (green open symbols), and 1.0 (blue crossed symbols). All data have been calculated for the initial number of initiators ($[I]_o$) equal to 100, the initial number of monomers ($[M]_o$) equal to 3125, and the initial monomer addition probability ($P_{a,o}$) of 1.0.

lattice was found to be homogeneous both for the bulk- and surface-initiated polymerizations throughout each simulation run. The latter observation is particularly important, as it states that the chain growth is not limited by the diffusion of the monomers. To further check for the effect of the monomer concentration on chain growth, we have performed additional sets of simulation with $[M]_o$ doubled (= 6250) and detected the exact same trends. While the data is not shown here, the results for the expected molecular weight for cases involving $[M]_o = 6250$ are presented in the Supporting Information. Hence, on the basis of these observations, we conclude that early chain termination observed in surface-initiated systems is the primary reason responsible for the increased polydispersity index relative to the bulk-initiated reactions. We will return to this point one more time later in the paper.

To gain more information about polymer concentration on the lattice, we first present selected data in the form of the number of monomers in the $X-Y$ plane as a function of Z, the lattice parameter that in the case of the surface-initiated polymerization represents the distance from the substrate. In Figure 9, we plot the in-plane number of monomers for $[I]_o = 100$, $[M]_o = 3125$, $P_{a,o} = 1.0$, and $P_t = 0.1$ for bulk- and surface-initiated polymerizations using open and closed symbols, respectively, for increasing monomer conversions equal to (a) 0.1, (b) 0.2, (c) 0.3, (d) 0.4, and (e) 0.5. While the average

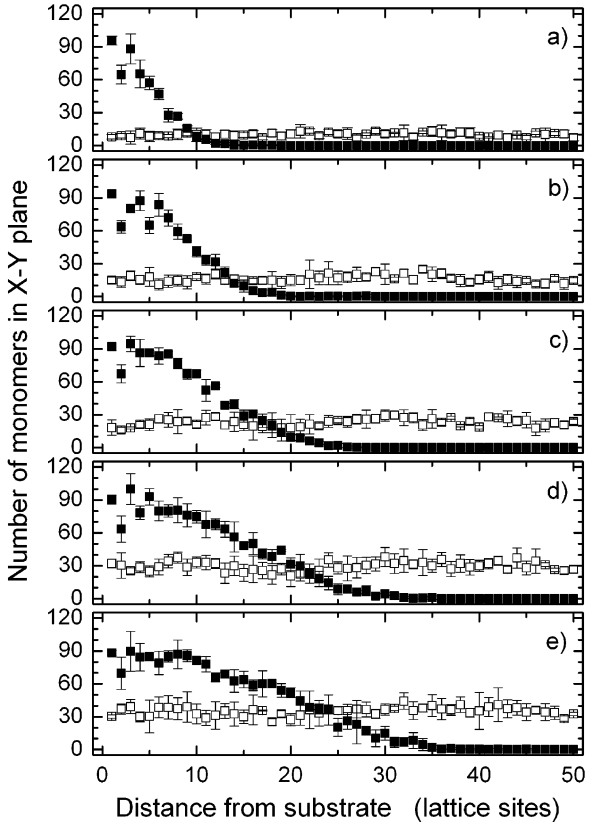

Figure 9. Number of monomers in the $X-Y$ plane as a function of the distance from the substrate for bulk (open symbols) and surface (closed symbols) initiated polymerization as a function of the monomer conversion equal to (a) 0.1, (b) 0.2, (c) 0.3, (d) 0.4, and (e) 0.5. The initial number of initiators ($[I]_o$) was equal to 100, the initial number of monomers ($[M]_o$) was equal to 3125, the initial monomer addition probability ($P_{a,o}$) was equal to 1.0, and the termination probability (P_t) was set to be 0.1. All data represent averages over three Monte Carlo runs.

number of monomers in the bulk-initiated reaction increases with increasing monomer conversion, in all cases, it does not depend on Z, as expected. In contrast, the in-plane number of monomers for the surface-initiated polymerization exhibits a "parabolic-like" profile predicted for polymer brushes.[72] With increasing monomer conversion, the in-plane concentration of polymer segments reaches a constant value close to the surface and decreases steadily at larger distances from the substrate. Because of the "excluded volume" interactions with its neighbors in the $X-Y$ plane, the "living" polymers continue to grow primarily in the direction away from the substrate. This behavior closely follows the trends in the average radius of gyration of all coils, reported earlier (cf. Figure 5). Recall that, for a given monomer conversion, the average chain dimensions in the X and Y directions are approximately the same, while the coil size in the Z direction is much larger. The distance to which the surface-initiated growing polymer extends from the surfaces depends on both $[I]_o$ and $[M]_o$. Because in our case the initiators are spaced equidistantly on the surface, the grafting density increases four times upon increasing $[I]_o$ from 25 to 100. In Figure 10, we plot the number of monomers in the $X-Y$ plane as a function of the distance from the surface for $P_{a,o} = 1.0$, $P_t = 0.1$ and various combinations of $[I]_o$ and $[M]_o$: (a) $[I]_o = 25$, $[M]_o = 3125$, (b) $[I]_o = 100$, $[M]_o = 3125$, (c) $[I]_o = 25$, $[M]_o = 6250$, and (d) $[I]_o = 100$, $[M]_o = 6250$. In all cases, the monomer conversion is set to 30%. The data in Figure 10 confirm the expected trends in the height of the profile as a function of $[I]_o$ and $[M]_o$. Namely, they demonstrate that the

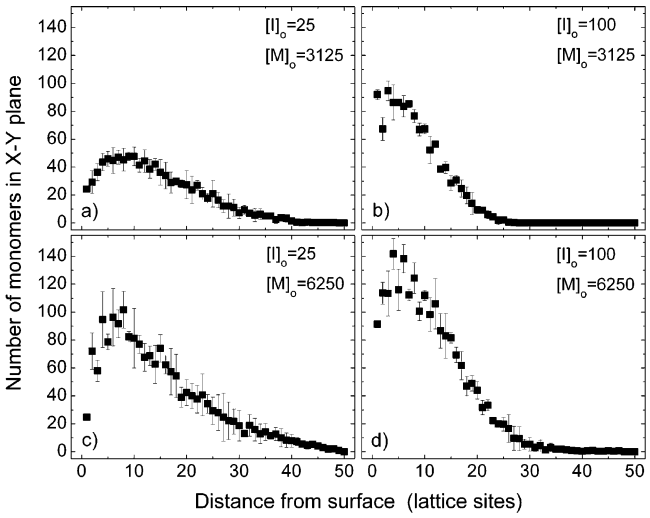

Figure 10. Number of monomers in the $X-Y$ plane as a function of the distance from the substrate for surface-initiated controlled radical polymerization for monomer conversion equal to 0.3 and the initial number of initiators ($[I]_o$) and the initial number of monomers ($[M]_o$) equal to: (a) $[I]_o = 25$, $[M]_o = 3125$, (b) $[I]_o = 100$, $[M]_o = 3125$, (c) $[I]_o = 25$, $[M]_o = 6250$, and (d) $[I]_o = 100$, $[M]_o = 6250$. In all simulations, the initial monomer addition probability ($P_{a,o}$) was equal to 1.0, and the termination probability (P_t) was set to be 0.1. All data represent averages over three Monte Carlo runs.

number of monomers in the $X-Y$ plane close to the surface increases by either: (1) keeping $[M]_o$ constant and increasing $[I]_o$ or by (2) keeping $[I]_o$ constant and increasing $[M]_o$. The profiles generated for $[I]_o = 25$ extend much further away from the surface than those for $[I]_o = 100$, as already discussed earlier. In fact, for the $[I]_o = 25$, $[M]_o = 6250$ case, even at this relatively low monomer conversion, the chains start to extend all the way to the other end of the lattice wall. Repeating the calculations with higher Z (= 100) confirm that this effect is very small at this monomer conversion, but becomes nonnegligible for higher monomer conversions.

We close by returning to the discussion of chain termination for bulk- and surface-initiated polymerizations. Earlier in the paper, we argued that, while for $[I]_o = 25$ the numbers of terminations for both bulk- and surface-initiated polymerization remained roughly the same, there was a rapid decrease in the number of terminated chains for surface-initiated polymerization with $[I]_o = 100$ relative to the bulk growth. The increased number of early terminations in the "grafting from" case was attributed to the close proximity of the growing polymers and their confinement, which resulted in their inability to avoid terminations. To visualize this effect, in Figures 11 and 12, we plot the center of mass positions of active (open symbols) and dead (closed symbols) polymers for $P_{a,o} = 1.0$, $P_t = 0.1$, various combinations of $[I]_o$, $[M]_o$, and at increased monomer conversions. The positions of the center of mass are visualized in the $Z-X$ plane; equivalent results are obtained by plotting the data in the $Z-Y$ plane. Figure 11 depicts the center of mass positions for bulk (a−c), upper panel) and surface (d−e), lower panel) polymerizations for $[I]_o = 25$, $[M]_o = 3125$, and monomer conversion of: (a, d) 0.1, (b, e) 0.2, and (c, f) 0.3. While for the bulk-initiated polymerization, the dead polymers are uniformly distributed throughout the lattice, the surface-initiated polymerization case contains dead chains that are confined close to the substrate, from which the polymerization initiated. Even more dramatic results are seen when the number of the initiators on the surface increases from 25 to 100. In Figure 12, we plot the center of mass positions for bulk (a−c), upper panel) and surface (d−e), lower panel) polymerizations for $[I]_o = 100$, $[M]_o = 3125$, and monomer conversion of: (a, d) 0.1, (b, e) 0.3, and (c, f) 0.5. As in the previous case, the dead chains are distributed uniformly throughout the lattice for the bulk-initiated polymerization. However, in the surface-initiated polymerization, the dead chains are located predominantly in the vicinity of the substrate. Hence, the data in Figures 11 and 12 visually substantiate our previous claims, namely that, in surface-initiated polymerizations a nonnegligible number of polymers gets rapidly terminated very close to the growing substrate even at

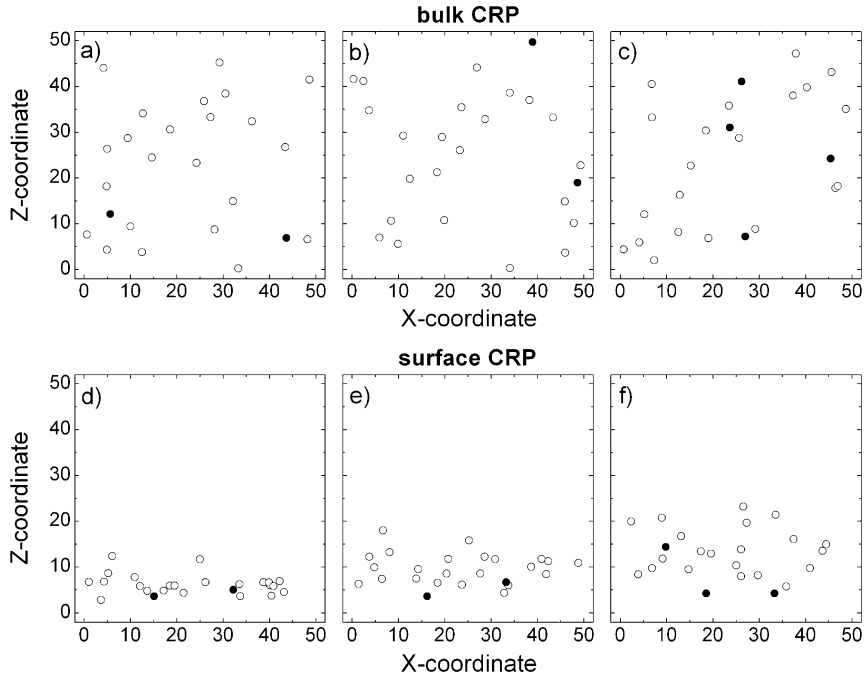

Figure 11. Positions of the center of mass of polymers grown via bulk (top panel) and surface (bottom panel) initiated polymerization for the initial number of initiators ($[I]_o$) equal to 25, the initial number of monomers ($[M]_o$) equal to 3125, the initial monomer addition probability ($P_{a,o}$) equal to 1.0, and the termination probability (P_t) equal to 0.1. The open and close symbols denote the center of mass position of active and dead polymers, respectively. The monomer conversion was: (a, d) 0.1, (b, e) 0.2, and (c, f) 0.3.

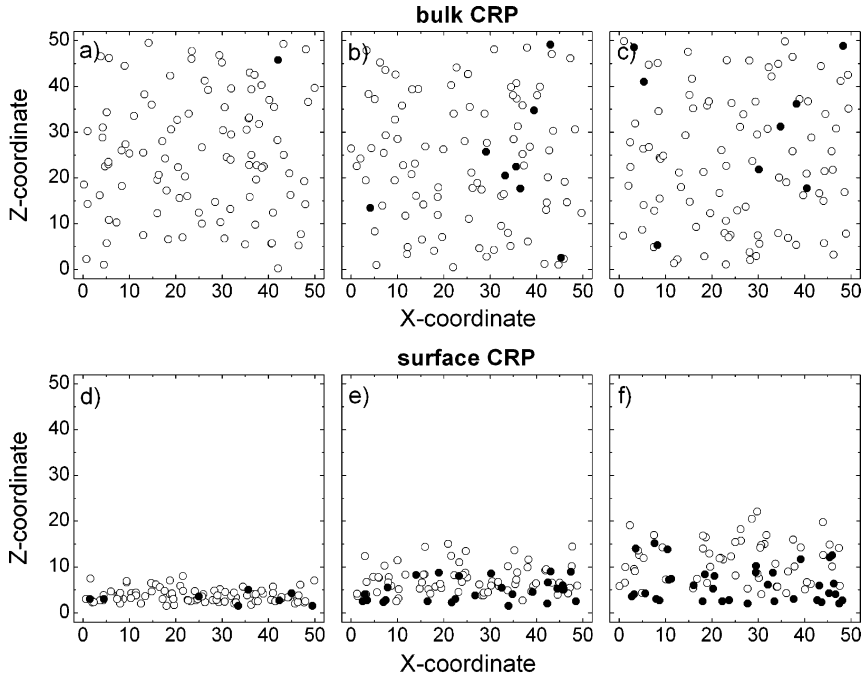

Figure 12. Positions of the center of mass of polymers grown via bulk (top panel) and surface (bottom panel) initiated polymerization for the initial number of initiators ($[I]_o$) equal to 100, the initial number of monomers ($[M]_o$) equal to 3125, the initial monomer addition probability ($P_{a,o}$) equal to 1.0, and the termination probability (P_t) equal to 0.1. The open and close symbols denote the center of mass position of active and dead polymers, respectively. The monomer conversion was: (a, d) 0.1, (b, e) 0.3, and (c, f) 0.5.

relatively small monomer conversions, an effect that gives rise to broader molecular weight distributions of surface-initiated chains relative to those polymerized in bulk.

Conclusions

The aim of this work was to gain insight into the mechanism of controlled/"living" radical polymerization in bulk and on flat substrates by utilizing a simple computational model based on Monte Carlo simulation. The effect of several molecular parameters affecting the properties of growing polymers was studied, including: the initial number of initiators ($[I]_o$), the initial number of monomers ($[M]_o$), the initiator activation probability (P_i, see Supporting Information for data), the initial probability of addition of a new monomer to a growing chain ($P_{a,o}$), the probability of terminating two "living" polymers (P_t), and the numbers of "living" polymers (FLP), and their lifetime (LT). Some observations reported in the paper are common for both bulk- and surface-initiated polymerization. First, the molecular weight of the polymers is always equal to the expected average molecular weight (M_p^*) given by $[M]_o/[I]_o$ for $P_t = 0$ (see Supporting Information) for all combinations of $[M]_o$ and $[I]_o$. Increasing P_t leads to larger deviations of the molecular weight from M_p^* and associated broadening of the molecular weight distribution, as indicated by an increase in the polydispersity index. Second, increasing $P_{a,o}$ improves the molecular weight distribution. Third, decreasing the lifetime of the "living" radicals leads to narrower molecular weight distributions of polymers. We also expected improvements in molecular weight distribution by lowering the fraction of "living" polymers in the total number of active, i.e., not terminated, macromolecules. However, no such effect has been detected. We attributed this to the finite size of our system, which cannot faithfully mimic real experimental conditions. Despite this drawback, the dependence of the polydispersity index on monomer conversion was found to exhibit the same qualitative features reported for real polymerization, i.e., an initial increase at very small monomer conversions followed by a decrease at higher monomer conversions. One of the goals of this work was to compare the results of polymerization initiated in bulk with that initiated from flat substrates. While the main trends reported above hold true for both types of polymerizations, some differences exist. The main disparity stems from confining the polymers growing from the surface, which in turn, gives rise to an increased number of early terminations, relative to the bulk-initiated polymerization, resulting in broader molecular weight distributions in surface-initiated polymers. This effect gets enhanced by increasing the grafting density of initiators on the surface.

Finally, let us comment on a comparison between the findings presented in this work and those published in previous theoretical papers that attempted to model experimental data using differential equations describing more sophisticated versions of Scheme 1. References 54−66 explored in detail the effects of the rate constants on the polymerization parameters, i.e., molecular weight and polydispersity index; good agreement was found between the measured and calculated quantities. Earlier in the paper, we have pointed out that, while the nature of our molecular model does not allow us to evaluate directly the values of the rate constants, correlations exist between the rate constants and the probabilities (or reaction and motion) used in the present model. The results obtained and presented in this work provide evidence that the two main attributes of CRPs, namely: (1) the linear dependence of the molecular weight on monomer conversion, and (2) an initial increase of the polydispersity index followed by its decrease as a function of the monomer conversion, can be faithfully reproduced. These effects are pronounced under conditions that correspond closely to the CRP process, namely, a small number of "active" radicals present at a given time during the polymerization, fast initiation, and a negligible termination. We thus are confident that, despite its simplicity, the present molecular model and the results discussed in this work provide valid molecular insight into controlled polymerizations. To this end, the results presented and discussed here may constitute a useful guide for experiments aiming at

understanding the structure of polymer brushes prepared by "grafting from" polymerizations.

Many questions still remain to be answered, however, that would provide more complete understanding of surface-initiated polymerizations. For instance, it would be interesting to model the free radical polymerization process. To do so, one would need to include the effect of chain transfer to the solvent, a feature that has not been included in the present work because it was assumed to play a negligible role in controlled radical polymerizations. This model can further be extended to other geometries, such as concave and convex, which would exhibit a different degree of confinement for both the initiators and the growing chains. To this end, polymerizations initiated from convex substrates, such as nanoparticles, should more closely follow the bulk-initiated growth. On the other side of the geometrical spectrum, polymerization from concave substrates, such as that carried out in pores, should lead to even stronger confinement effects and hence fewer controlled polymerizations. Some experiments along these lines exist, and our preliminary calculations seem to follow the expected and observed trends. These will be reported in a separate publication. Finally, in this model, we worked with the NVT ensemble. It would be interesting to switch to a system where, instead of maintaining the total number of species constant, we keep constant the chemical potential of the free monomers. That would effectively correspond to situations involving a very large monomer excess, and as such would even more closely represent real experimental conditions.

Glossary of Terms and Used Variables

active polymer = polymer that is not terminated; it can either be "living" or dormant. This polymer can either move or can potentially be activated. When activated, it becomes "living" polymer. This polymer contributes to increasing the degree of polymerization of the assembly of chains.

dead polymer = polymer that has been terminated. Once dead, it cannot be reactivated. It can only move (if selected).

living polymer = polymer that is "living", i.e., an active polymer that can undergo either propagation or termination. The propagation takes place with a certain "living" radical reaction probability, P_a; hence, a "living" radical does not always undergo reaction. The probability that a "living" radical can react depends on the instantaneous concentration of free (= unreacted) monomers.

macroinitiator = initiator or a living polymer (= polymer in its "living" state) capable of propagation and/or termination

FLP = fraction of living polymers of the total number of polymers (e.g., 2%)

$[I]_o$ = initial number of initiators

LT = lifetime of living polymers; that is, the number of MCS for which an active polymer that is a member of the FLP can propagate

M_n = number-average molecular weight

M_w = weight-average molecular weight

$[M]_o$ = initial number of free monomers

$[M]_t$ = number of free monomers at time t

$[P]_t$ = number of existing polymers at time t

$[P]_{act,t}$ = number of active polymers (macroinitiators) at time t

$[P]_{liv,t}$ = number of "living" polymers (macro-initiators) at time t

τ_{lt} = lifetime of a "living" polymer (in MC cycles); this is, the maximum number of MCS for which the active polymer remains "living" before it is deactivated. Once the polymer gets terminated, its state changes from active to dead.

τ_{act} = active time of a (macro)initiator; this is, the time during which the (macro)initiator can add one more monomer

τ_{dorm} = dormant time of a (macro)initiator (= the total lifetime of an active (macro)initiator)

τ_{cycle} = time of the "dormant/living" cycle

P_a = probability of adding a monomer to a growing chain ($= P_{a,o}\text{-}[M]_t/[M]_o$)

$P_{a,o}$ = initial probability of adding a monomer to a growing chain

P_i = initiator activation (= initiation) probability

P_m = probability of polymer motion $P_m = 1 - \sum([M]_t)/\sum([P]_t + [M]_t)$

P_r = polymer reaction vs motion probability (set to $P_r = 0.5$)

P_t = probability of termination of living polymers

$P_{t,c}$ = probability of termination of living polymer via combination (set to $P_{t,c} = 0.5$)

PDI = polydispersity index ($= M_w/M_n$)

$R_{g,x}$ = average radius of gyration of polymer in the X direction on the lattice

$R_{g,y}$ = average radius of gyration of polymer in the Y direction on the lattice

$R_{g,z}$ = average radius of gyration of polymer in the Z direction on the lattice

R_g = average radius of gyration of polymer

Acknowledgment. This work was supported by the National Science Foundation and the Camille & Henry Dreyfus Foundation. I thank Dr. Petr Vlček (Institute of Macromolecular Chemistry in Prague, Czech Republic) for fruitful discussions about controlled radical polymerization and Mr. Erik Santiso (NC State University) and Dr. Andrew J. Schultz (SUNY Buffalo) for discussions pertaining to Monte Carlo simulation. Finally, I thank Professor Igal Szleifer (Purdue University) for fruitful discussion and encouragement.

Supporting Information Available: Additional data pertaining to the molecular weight of polymers, whose growth was simulated using the Monte Carlo model described in the main text; values of the average molecular weight of the polymers for various combinations of the initial number of the initiators, ($[I]o$), the initial number of monomers ($[M]o$), the initiator activation efficiency (P_i), the initial probability of addition of a new monomer to a growing chain ($P_{a,o}$), the probability of terminating two living polymers (P_t), and the numbers of living polymers (FLP) and their life time (LT). This material is available free of charge via the Internet at http://pubs.acs.org.

References and Notes

(1) Matyjaszewski, K. General Concepts and History of Living Radical Polymerization. In *Handbook of Radical Polymerization*; Matyjaszewski, K., Davis, T. P., Eds.; John Wiley & Sons: New York, 2002; Chapter 8, p 361.
(2) Qiu, J.; Charleux, B.; Matyjazsewski, K. *Prog. Polym. Sci.* **2001**, *26*, 2083.
(3) Ando, T.; Kato, M.; Kamigaito, M.; Sawamoto, M. *Macromolecules* **1996**, *29*, 1070.
(4) Matyjaszewski, K.; Patten, T. E.; Xia, J. H. *J. Am. Chem. Soc.* **1997**, *119*, 674.
(5) Brittain, W. J., Advincula, R., Rühe, J., Caster, K., Eds. *Polymer Brushes*; Wiley & Sons: New York, 2004.
(6) Patten, T. E.; Matyjaszewski, K. *Adv. Mater.* **1998**, *10*, 901 and references therein.
(7) Matyjaszewski, K.; Xia, J. *Chem. Rev.* **2001**, *101*, 2921.
(8) Zhao, J.; Brittain, W. J. *Prog. Polym. Sci.* **2000**, *25*, 677.
(9) Edmondson, S.; Osborne, V. L.; Huck, W. T. S. *Chem. Soc. Rev.* **2004**, *33*, 14.
(10) Radhakrishnan, B.; Ranja, R.; Brittain, W. J. *Soft Mater.* **2006**, *2*, 386.
(11) Matyjaszewski, K.; Miller, P. J.; Shukla, N.; Immaraporn, B.; Gelman, A.; Luokala, B. B.; Siclovan, T. M.; Kickelbick, G.; Vallant, T.; Hoffmann, H.; Pakula, T. *Macromolecules* **1999**, *32*, 8716.
(12) Kong, X.; Kawai, T.; Abe, J.; Iyoda, T. *Macromolecules* **2001**, *34*, 1837.
(13) Kim, J. B.; Huang, W.; Bruening, M. L.; Baker, G. L. *Macromolecules* **2002**, *35*, 5410.
(14) Husemann, M.; Mecerreyes, D.; Hawker, C. J.; Hedrick, J. L.; Shah, R.; Abbott, N. L. *Angew. Chem., Int. Ed.* **1999**, *38*, 647.
(15) Shah, R.; Mecerreyes, D.; Husemann, D.; Rees, I.; Abbott, N. L.; Hawker, C. J.; Hedrick, J. L. *Macromolecules* **2000**, *33*, 597.
(16) Jeon, N. L.; Choi, I. S.; Whitesides, G. M.; Kim, N. Y.; Laibinis, P. E.; Harada, Y.; Finnie, K. R.; Girolami, G. S.; Nuzzo, R. G. *Appl. Phys. Lett.* **1999**, *75*, 4201; Kim, N.; Jeon, N. L.; Choi, I. S.; Takami,

S.; Harada, Y.; Finnie, K. R.; Girolami, G. S.; Nuzzo, R. S.; Whitesides, G. M.; Laibinis, P. E. *Macromolecules* **2000**, *33*, 3793.
(17) de Boer, B.; Simon, H. K.; Werts, M. P. L.; van der Vegte, E. W.; Hadziioannou, G. *Macromolecules* **2000**, *33*, 349.
(18) Ghosh, P.; Lackowski, W. M.; Crooks, R. M. *Macromolecules* **2001**, *34*, 1230.
(19) Jones, D. M.; Huck, W. T. S. *Adv. Mater.* **2001**, *13*, 1256.
(20) Hyun, J.; Chilkoti, A. *Macromolecules*, **2001**, *34*, 5644.
(21) Osbourne, V. L.; Jones, D. M.; Huck, W. T. S. *Chem. Commun.* **2002**, 1838.
(22) Wu, T.; Efimenko, K.; Genzer, J. *J. Am. Chem. Soc.* **2002**, *124*, 9394.
(23) Wu, T.; Efimenko, K.; Vlček, P.; Šubr, V.; Genzer, J. *Macromolecules* **2003**, *36*, 2448.
(24) Wu, T.; Genzer, J.; Gong, P.; Szleifer, I.; Vlček, P.; Šubr, V. Behavior of Surface-Anchored Poly(acrylic acid) Brushes with Grafting Density Gradients on Solid Substrates. In *Polymer Brushes*; Brittain, W. J., Advincula, R., Rühe, J., Caster, K., Eds.; Wiley & Sons: New York, 2004.
(25) Tomlinson, M. R.; Genzer, J. *Macromolecules* **2003**, *36*, 3449.
(26) Xu, C.; Wu, T.; Bateas, J. D.; Drain, C. M.; Beers, K. L.; Fasolka, M. J. *Appl. Surf. Sci.* **2006**, *252*, 2529.
(27) Tomlinson, M. R.; Genzer, J. *Chem. Commun.* **2003**, 1350.
(28) Tomlinson, M. R.; Genzer, J. *Langmuir* **2005**, *21*, 11552.
(29) Xu, C.; Wu, T.; Mei, Y.; Drain, C. M.; Batteas, J. D.; Beers, K. L. *Langmuir* **2005**, *21*, 11136.
(30) Xu, C.; Barnes, S. E.; Wu, T.; Fischer, D. A.; DeLongchamp, D. M.; Batteas, J. D.; Beers, K. L. *Adv. Mater.* **2006** in press.
(31) Bhat, R. R.; Tomlinson, M. R.; Genzer, J. *Macromol. Rapid Commun.* **2004**, *25*, 270.
(32) Bhat, R. R.; Chaney, B. N.; Rowley, J.; Liebmann-Vinson, A.; Genzer, J. *Adv. Mater.* **2005**, *17*, 2802.
(33) Bhat, R. R.; Tomlinson, M. R.; Genzer, J. *J. Polym. Sci., Polym. Phys.* **2005**, *43*, 3384 and references therein.
(34) Bhat, R. R.; Tomlinson, M. R.; Wu, T.; Genzer, J. *Adv. Polym. Sci.* **2006**, *198*, 51 and references therein.
(35) von Werne, T.; Patten, T. E. *J. Am. Chem. Soc.* **1999**, *121*, 7409.
(36) von Werne, T.; Patten, T. E. *J. Am. Chem. Soc.* **2001**, *123*, 7497.
(37) Perruchot, C.; Khan, M. A.; Kamitsi, A.; Armes, S. P.; von Werne, T.; Patten, T. E. *Langmuir* **2001**, *17*, 4479.
(38) Carrot, G.; Diamanti, S.; Manuszak, M.; Charleux, B.; Vairon, I. P. *J. Polym. Sci., Part A: Polym. Chem.* **2001**, *39*, 4294.
(39) Bontempo, D.; Tirelli, N.; Masci, G.; Crescenzi, V.; Hubbell, J. A. *Macromol. Rapid Commun.* **2002**, *23*, 418.
(40) Tsujii, Y.; Ejaz, M.; Sato, K.; Goto, A.; Fukuda, T. *Macromolecules* **2001**, *34*, 8872.
(41) Yoon, M. S.; Ahn, K. H.; Cheung, R. W.; Sohn, H.; Link, J. R.; Cunin, F.; Sailor, M. J. *Chem. Commun.* **2003**, 680.
(42) Bruening, M. L.; Miller, M. D.; Balachandra, A.; Huang, W.; Baker, G. L. *Polym. Prepr.* **2003**, *44*, 467.
(43) Miller, M. D.: Baker, G. L.; Bruening, M. L. *J. Chromatogr.* A **2004**, *1044*, 323.
(44) Dai, J. H.: Baker, G. L.; Bruening, M. L. *Anal. Chem.* **2006**, *78*, 135.
(45) Akgun, B.; Boyes, S. G.; Granville, A. M.; Brittain, W. J.; Foster, M. D. *Polym. Prep.* **2003**, *44*, 514.
(46) Jones, D. M.; Brown, A. A.; Huck, W. T. S. *Langmuir* **2002**, *18*, 1265.
(47) Liu, Y.; Klep, V.; Luzinov, I. *Polym. Prepr.* **2003**, *44*, 564.
(48) Liu, Y.; Klep, V.; Zdyrko, B.; Luzinov, I. *Langmuir* **2004**, *20*, 6710.
(49) Liu, Y.; Klep, V.; Zdyrko, B.; Luzinov, I. *Langmuir* **2005**, *21*, 11806.
(50) Bao, Z.; Bruening, M. L.; Baker, G. L. *Macromolecules* **2006**, *39*, 5251.
(51) Kim, J. B.; Huang, W.; Miller, M. D.; Baker, G. L.; Bruening, M. L. *J. Polym. Sci., Part A: Polym. Chem.* **2003**, *41*, 386.
(52) Colombani, D. *Prog. Polym. Sci.* **1997**, *22*, 1649.
(53) Zhu, S. *J. Polym. Sci., Polym. Phys.* **1999**, *37*, 2692.
(54) Yan, D.; Jiang, H.; Fan, X. *Macromol. Theory Simul.* **1996**, *5*, 333.
(55) Fischer, H. *J. Polym. Sci., Polym. Chem.* **1999**, *37*, 1895.
(56) Zhu, S. *Macromol. Theory Simul.* **1999**, *8*, 29.
(57) He, J.; Li, L.; Yang, Y. *Macromol. Theory Simul.* **2000**, *9*, 463.
(58) Zhang, M.; Ray, W. H. *Ind. Eng. Chem. Res.* **2001**, *40*, 4336.
(59) Zhang, M.; Ray, W. H. *Macromol. Symp.* **2002**, *182*, 169.
(60) Zhang, M.; Ray, W. H. *J. Appl. Polym. Sci.* **2002**, *86*, 1630.
(61) Delgadillo-Velázquez, O.; Vivaldo-Lima, E.; Quintero-Ortega, I. A.; Zhu, S. *AICHE J.* **2002**, *48*, 2597.
(62) Shen, Y.; Zhu, S. *AICHE J.* **2002**, *48*, 2609.
(63) Wang, A. R.; Zhu, S. *J. Polym. Sci., Polym. Chem.* **2003**, *41*, 1553.
(64) Wang, A. R.; Zhu, S. *Macromol. Theory Simul.* **2003**, *12*, 196.
(65) Bousou, B.; Pflueger, F. *Macromol. Theory Simul.* **2003**, *12*, 243.
(66) Wang, A. R.; Zhu, S. *Macromol. Theory Simul.* **2003**, *12*, 663.
(67) Leigh, S.; Liu, G.; Patten, T. E. *Polym. Prepr.* **2005**, *46*, 3.
(68) Carmesin, I.; Kremer, K. *Macromolecules* **1988**, *21*, 2819.
(69) Binder, K. *Monte Carlo and Molecular Dynamics Simulations in Polymer Science*; Oxford University Press: New York, 1995; p 17.
(70) This is one place where further improvements can be made. The value of P_m can be based on some physical state of the system, i.e., solution viscosity. Highly viscous systems will hinder the motion of mainly polymers and to some extent also monomers and hence will exhibit a higher reaction probability. P_m will be constantly updated throughout the simulation.
(71) The radius of gyration (R_g) values have been calculated over the entire ensemble. While each individual coil adopts a shape of a slightly elongated ellipsoid (see, for instance, Szleifer, I. *J. Chem. Phys.* **1990**, *92*, 6940; Szleifer, I.; O'Toole, E. M.; Panagiotopoulos, A. Z. *J. Chem. Phys.* **1992**, *97*, 6802; Zifferer, G.; Olaj, O. F. *J. Chem. Phys.* **1994**, *100*, 636 and references therein), averaging the dimensions of all coils present in the ensemble gives a value of R_g that is the same in all direction along the lattice. This result further justifies that all coils have, on average, the same dimension, regardless of their local orientation.
(72) Milner, S. T. *Science* **1991**, *251*, 905.

MA061155F